

THE “PISCO” SPECKLE CAMERA AT PIC DU MIDI OBSERVATORY¹

J.-L. Prieur*, L. Koechlin*, C. André*, G. Gallou*, C. Lucuix*

*Observatoire Midi-Pyrénées, 14, Avenue E. Belin, F-31400 Toulouse, France.

Abstract:

We present a new speckle camera designed and built at Observatoire Midi-Pyrénées. This focal instrument has been used for two years with the 2-meter Bernard Lyot Telescope of Pic du Midi observatory. It can be set in various operating modes: full pupil imaging, masked-pupil imaging, spectroscopy, wave-front sensor and stellar coronagraphy, hence its name “PISCO” (“Pupil Interferometry Speckle COronagraph”). Restored images of double and triple stars have demonstrated its capabilities in providing close to diffraction limited images (0.06" in V). PISCO has been fully tested and is now ready to be used by the whole astronomical community.

1. Introduction

This speckle camera was designed and built between 1991 and 1994 by the “Aperture synthesis team” of Observatoire Midi Pyrénées (OMP), as a new focal instrument for the 2 meter Télescope Bernard Lyot (TBL) at Pic du Midi. The aim was to take advantage of the good seeing quality of that site.

The optical design was chosen such that a pupil plane would be accessible and pupil masks could be put into it, to allow for aperture synthesis experiments and simulate telescope arrays such as the ESO VLTI (European Southern Observatory Very Large Telescope in the Interferometric mode) or others. This speckle camera thus provides appropriate experimental tools for the investigation of image restoration techniques with the optical telescope interferometric networks that are currently being built and operated around the world (CHARA, COAST, G3T, IOTA, NPOI, PTI, SUSI, etc, see *f.i.* *Astronomical Interferometry*, Proceedings of SPIE, Vol. 3350, Kona, 20-28/03/98)

In the following we present an overview of PISCO and its optical concept (§2). Then we introduce the various operative modes and illustrate them with observational results (§3). The detectors that have been used with PISCO are presented in §4. In §5, we discuss the current performances of the instrument in relation with the physical limitations of the speckle techniques and the image restoration methods. In §6 we briefly describe the on-going scientific programs which use PISCO, and conclude about the use of a speckle camera in the current context of new high angular resolution techniques.

2. The PISCO speckle camera

Compared to other speckle cameras (Blazit *et al.*, 1977, Breckinridge *et al.* 1979, Strittmater, 1980, Beckers *et al.*, 1983, Foy, 1988a) our instrument presents the advantage of a versatility and a full remote control of all its operating modes. PISCO offers thus a wide range of possibilities with fast switching between modes (less than one minute), allowing an optimal use of the seeing conditions.

2.1. Description

The general layout is shown in Fig. 1. The external mechanical structure is a rectangular box of 100×40×36 cm³ which is mounted at the Cassegrain focus of the telescope (Fig. 2).

The input image plane (I1) of the telescope is located 200 mm downstream from the front flange of PISCO (this value is easily adaptable for the 3.6 m CFH or ESO telescopes). The

¹Based on observations made at Télescope Bernard Lyot, Pic du Midi, France

converging input beam is transformed into a parallel beam by the collimating lens (L2), then focused into the image plane (I2) by the lens (L3).

Lens (L4) magnifies this image and projects it to the detector faceplate. The focal length of (L4) can be selected with the wheel GR that bears a series of eyepieces and microscope objectives. A magnification of at least 20 mas/pixel is needed to obtain a good sampling for speckle observations at the TBL while a lower magnification is used for field acquisition.

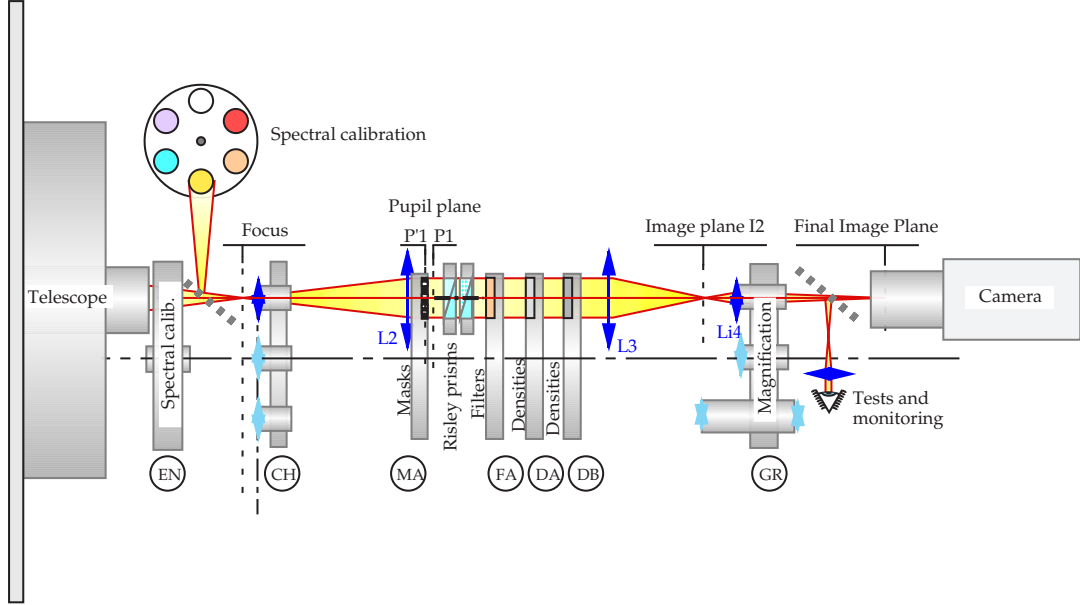


Figure 1: Optical diagram of PISCO.

Filters (wheels FA and FB) allow selecting the desired wavelength range while neutral densities (wheels DA and DB) are used to adjust the light level to the (generally poor) dynamic range of the photon-counting detectors (see §4). As will be explained in § 2.2, a set of Risley prisms correct for the atmospheric chromatic dispersion.

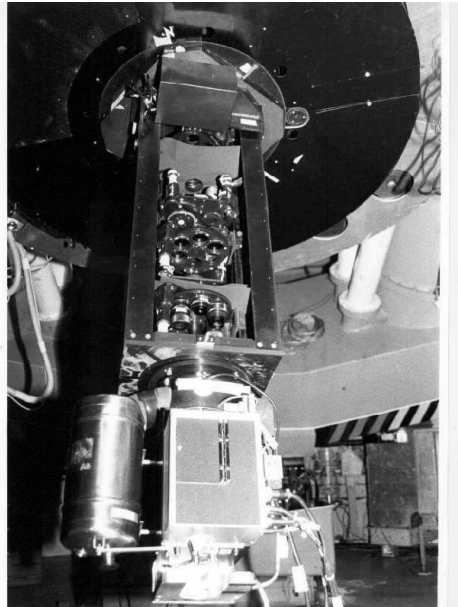


Figure 2: PISCO and photo-counting detector CP40 at the TBL.

When a field lens is selected (wheel CH), the pupil plane is located in the plane of the wheel MA, where pupil masks are available for coronagraphy (§3.3) or multi-aperture interferome-

try (§3.2). If low dispersion spectroscopy (§3.4) is wanted, a grism can be put into the parallel beam (wheel FA). Wavefront analysis is also possible with a Hartman sensor by selecting a microlens array in the wheel MA, and the pupil imaging mode in wheel GR.

PISCO can then be seen as an optical bench on which mounts and wheels can freely move and rotate. This concept allows a great flexibility for future instrumental developments. All instrumental functions, including wheel positioning and control of the Risley prisms are monitored by a microprocessor and remotely accessible via a RS232 link.

One of us (J.-L. Prieur) has developed a program in the PC/Window environment to facilitate the remote control of PISCO. All the basic functions are available (Fig. 3) with mouse-driven menus. The program controls in real time the atmospheric dispersion correction according to the telescope position, the filter and the atmosphere parameters (§2.2). A log file is also produced at the end of each night with the PISCO setup parameters of all the exposures taken during that night.

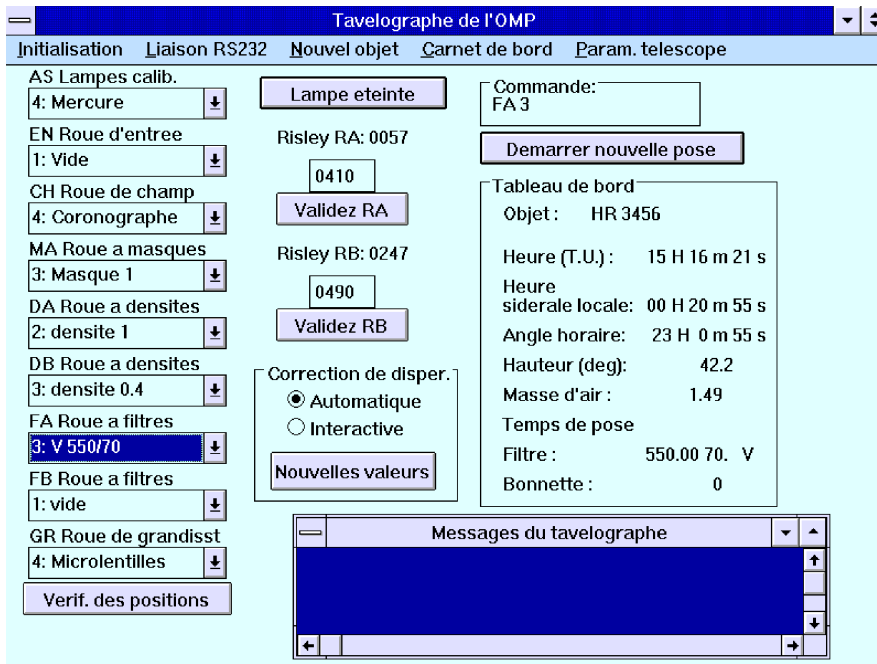


Figure 3: Main panel of the program which controls the speckle camera PISCO.

PISCO was primarily designed to be used at the Cassegrain focus of TBL, but it has also been made mechanically and optically compatible with the Cassegrain foci of the Canada-France-Hawaii (CFH) and European Southern Observatory (ESO) 3.6-m telescopes.

2.2. Atmospheric dispersion correction with Risley prisms

For an astronomical object observed from the ground at an elevation different from zenith, the atmosphere behaves as a dispersive prism (see f.i., Simon, 1966). Polychromatic images are spread into a small vertical spectrum. For instance, for a 250 nm bandwidth centered at 500 nm, the typical atmospheric dispersion is 1" for an elevation $h = 60^\circ$ and 2" for $h = 30^\circ$.

In PISCO, the atmospheric dispersion is corrected with "Risley prisms," which consist in two identical sets of prisms (Breckinridge *et al.* 1979, Walner, 1990) that can be rotated to produce a tunable chromatic dispersion both in amplitude and direction (Fig. 4a).

Each set is made of two prisms of different dispersion law and roof angles, placed in an upside-down position. These prisms have been designed to have a null mean deviation, and a dispersion allowing atmospheric correction from the zenith down to an elevation of 30° for the blue domain which is the most defavorable (B filter, centered at 450 nm with a 70 nm

bandwidth). We used the same combination of Shott glasses (F4, SK10) as the one used for the Kitt Peak speckle camera (Breckinridge *et al.*, 1979). Wallner (1990) found other combinations which are closer to the atmospheric dispersion curve but we chose the Kitt Peak combination because of its low cost and sufficient efficiency for our purpose. Our Risley prisms reduce the residual dispersion down to a level smaller than 0.01" for every location of the object in the sky above an elevation of 30°, with the 70 nm bandpass B filter which is small compared to the diffraction limit of 0.05" in B at the TBL.

During the observations, a specially designed program (already mentioned in §2.1) computes the elevation of the star and the corresponding atmospheric dispersion using J.C. Owens' model of atmosphere (Owens, 1967, formulae 29–31). The Risley prisms are then dynamically rotated during data acquisition to compensate for the atmospheric dispersion.

3. The observation modes

PISCO can be used in various modes which are selected during the observations. Switching from one mode to another takes a few mouse clicks and less than one minute for the motors to set the wheels.

3.1. Full pupil speckle imaging

In this mode, no pupil masks are used and a high magnification is selected with wheel GR (Fig. 1). It corresponds to the “conventional” way of observing in speckle interferometry. Most speckle cameras (Breckinridge *et al.* 1979, Strittmater, 1980, Foy, 1988a). offer only this possibility – or would require many optical changes with a full re-calibration of the instrument for other operating modes –. By applying bispectral techniques (§5.2), we have obtained images with an angular resolution close to the diffraction limit of the telescope (Fig. 4b).

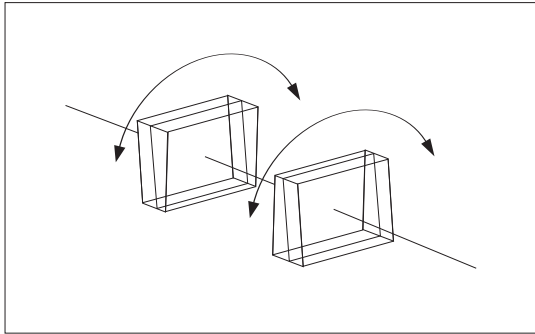


Figure 4a. Risley Prisms to correct for the atmospheric dispersion.

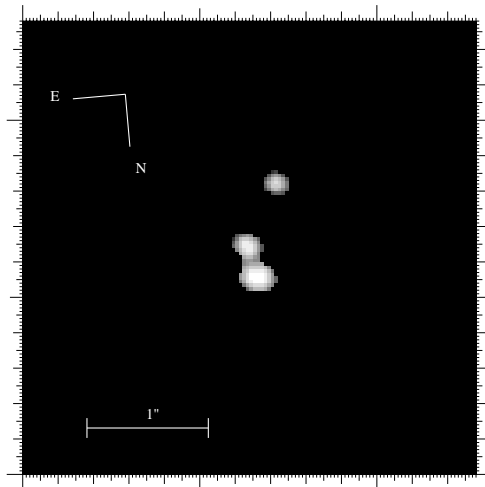


Figure 4b. Full pupil speckle imaging: restored image of the triple star 2 Cam, at the TBL.

The full pupil is used and the optical transfer function (OTF) corresponds to that of the telescope, and we shall see in the following that another OTF may be preferred. For instance, the diffraction pattern of the telescope spider may pollute the final image and hinder the detection of faint objects in the vicinity of a bright one.

Another drawback of this OTF is that low spatial frequencies dominate the transfer function. In photon counting mode mode, the few available photons are then mainly spread in the (less useful) low frequencies.

As the limited dynamic range of detectors such as the CP40 imposes the use of neutral densities to reduce the photon flux for bright objects to only a few hundreds per frame (§4), they always work in photon counting mode. This limits the performances of the restoration methods even for bright objects. This is the reason why the next mode could be preferred in that case.

3.2. Masked pupil speckle imaging and aperture synthesis

By inserting masks into the pupil plane (P1) (cf. Fig. 1), the pupil function (and thus the OTF) can be modified as desired. For instance the spider diffraction pattern can be removed by placing a Lyot’s mask or a four-hole mask which carefully avoids the shadow of the spider (see §3.3), and telescope arrays can be simulated by placing a mask with appropriately located small holes.

Pupil masks allow to select a sub-sample of spatial frequencies and more accurately measure the corresponding complex visibilities since they will be less attenuated (as the overlap of the fringes is lower); hence, a better use of the maximum number of photons allowed by the detector. The price to pay is to perform an interpolation in the Fourier space (aperture synthesis, see methods in §5.1) and complementary observations to make the process more robust in the case of complex objects.

We made 3 pupil masks by drilling 0.7 mm holes into a 5-cm metallic disk, according to some of the complementary non-redundant networks from Golay (1971). They are displayed in Fig. 5 with the corresponding (u, v) coverage. A successful image of HR 8652 was restored using these masks and the aperture synthesis method from Lannes (1989, 1991) and Anterrieu (1992). These method would work with any other configuration – there is no need for complementary networks –. We chose these masks because the corresponding (u, v) coverage (Fig. 5) was rather compact with only small gaps, which makes image restoration more robust.

The main drawback is a lower limiting magnitude in the case of small holes, and this method can only be used for objects with $V < 8$ at the TBL.

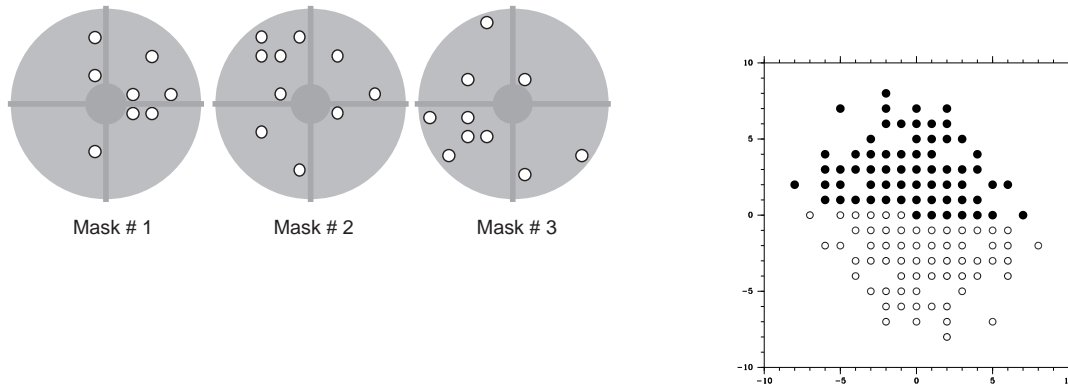


Figure 5: Set of pupil masks available in PISCO (left) and corresponding (u, v) coverage (right).

3.3. Coronagraphic mode

PISCO can be used as a Lyot’s coronagraph by putting adequate masks m_1 in the entrance image plane (I1) and m_2 in the pupil plane (P1) (wheels EN and MA of Fig. 1). This mode was successfully tested in 1994 with long integrations on a conventional CCD detector. Speckle imaging from short-exposed frames has little interest in this mode since the obturation of

the mask m_1 in (I1) needs to be quite large (a few times the FWHM seeing) to hide most of the brightness of the central target. This mode would take its real advantage with adaptive optics and a small obturation of m_1 , to investigate closer to the target (see f.i., some recent developments with a phase mask in the image plane, Roddier & Roddier, 1997).

A four-hole pupil mask can also be used to suppress the diffraction image of the spider of the telescope. This reduces the diffusion of a bright object and allows the detection of a possible faint close companion or stellar envelopes, as seen in Fig. 6. The stellar profile is more concentrated when putting this mask. If we normalize the profiles with the central value, the level of the wings has been reduced by a factor larger than 3.

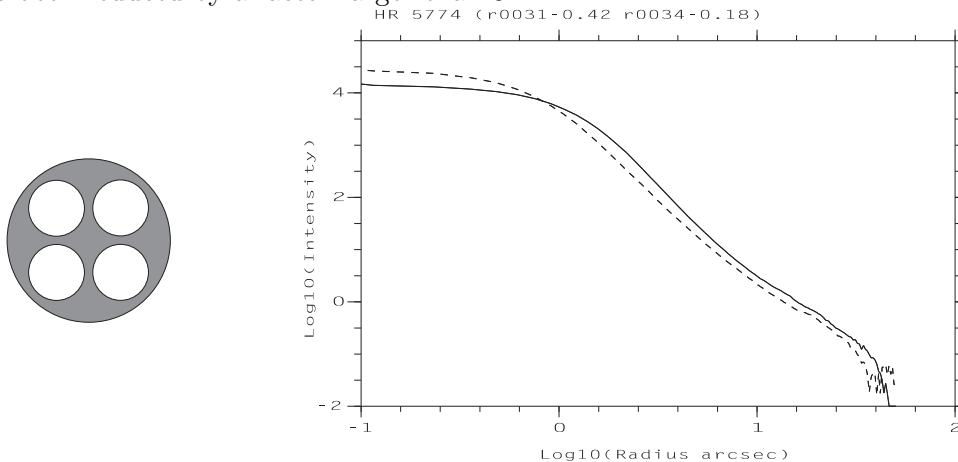


Figure 6: Pupil mask used to remove the diffraction pattern of the spider in the coronagraphy mode (left), and profile of the star HD5774 (right) with (dashed line) and without (solid line) that mask.

3.4. High angular resolution spectroscopy

Some authors have already shown the feasibility of speckle spectroscopy (Weigelt *et al.*, 1991, Kuwamura *et al.*, 1992) which has a great interest for the individual study of binary stars or for determining the physical nature of fine details found in speckle imaging. Two possibilities have been used: spectroscopy with or without a slit in the entrance image plane.

- Both the Hokudai speckle camera at the Okayama 188 cm telescope and the Steward Observatory speckle camera with the spectroscopy module at KPNO used by Kuwamura *et al.*, 1992, worked in *objective prism spectroscopy mode*, i.e., slitless spectroscopy. In this mode, the resolution is not fixed and changes as the seeing varies. The spectral calibration is rather difficult to perform since it depends upon the position of the object in the field. But the main advantage is that all the incoming light is used, without any loss.

- Weigelt *et al.*, 1991, proposed a slit spectroscopy setup which allows a high spectral resolution and a fixed spectral calibration. This is the option we chose because we wanted to be able to do stellar classification of the components of binary stars and work with a good spectral calibration. The main drawback is a loss of sensitivity due to a rejection of the light by the entrance slit.

PISCO can be easily converted to a spectrograph by selecting the grism in the wheel FA and a slit in the wheel EN in the entrance image plane (I1) (Fig. 1). It then provides a low dispersion spectrographic mode with a spectral range of 350–500 nm, and a spectral resolution of ~ 300 with a slit of 0.7". This range was chosen to allow stellar classification of close binaries with the hydrogen Balmer series. Unfortunately, the atmospheric turbulence is stronger in the blue domain, which make images more difficult to restore. The wavelength calibration can be performed with calibration spectral lamps in wheel AS (Halogen, Argon, Neon and Xenon lamps).

Quick switching between imaging and spectroscopy is possible since this mode can be remotely selected by rotating the wheels. The observing procedure is the following:

- obtain the autocorrelation of the binary star in the full pupil mode (cf., §3.1) and measure the rotation angle to align the slit on the direction of the two components.
- rotate the telescope flange supporting PISCO and center the object on the slit.
- switch to the spectroscopic mode and record the data.

Restoration of high angular resolution information in the direction of the entrance slit is then done by applying one-dimensional speckle imaging techniques to each monochromatic image of the slit (see §5.2).

The first spectroscopic observations were made in 1995. Unfortunately the poor seeing conditions and the low dynamic range of the detector did not allow us to restore high resolution images. We simply obtained long integration spectra (Fig 7) and calibrated the whole instrument with known stars.

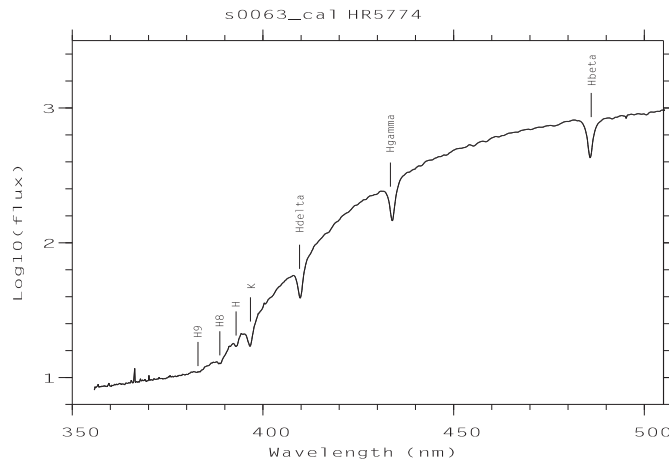


Figure 7: First spectrum obtained with PISCO (HD 5774).

3.5. Wavefront analyzer

The atmospheric wavefront can be sensed with the Shack-Hartman method (Roggeman *et al.*, 1997), by putting a microlens array into the pupil plane (P1) and a specific imaging lens in the GR wheel, (cf. Fig. 1). Each microlens has a diameter of 0.7 mm which corresponds to 20 cm on the pupil at the TBL and 10 cm at the 3.6 m CFH or ESO telescopes.

The SCIDAR (SCintillation Detection And Ranging) technique (Vernin & Roddier, 1973) which consists in analysing the images of the pupil brightness lit by two stars to measure the wind speed and the altitude of the turbulence layers, could also be applied with PISCO. In that case, fast detectors operating at frequencies larger than 200 Hz (such as the PAPA or the RANICON cameras, cf. §4) are needed to "freeze" the turbulence.

4. The detectors

PISCO has been used with a wide range of detectors. Actually, the qualities of the detector mainly condition the performances of the image restoration process. A good knowledge of the limitations of the detector is essential to elaborate a strategy of observation and obtain valid measurements. Here we describe the detectors that we have already tested on PISCO. For a wider information about the detectors used in the field of optical speckle interferometry, see for instance a review in Cuby (1988), Richard *et al.*, (1990) or Cuby *et al.*, (1990).

4.1. The CP40-INSU detector

The first CP40 detector was designed at CERGA for interferometry observations by A. Blazit (Blazit, 1976, 1987). It is a two-stage intensified CCD camera followed by a photon analyzer

which computes the coordinates of the photo-events (Foy, 1988b). The field is covered by a mosaic of 4 CCD's, 288×384 pixels each. We actually used the duplication of this prototype, financed by INSU to make it available to the French astronomical community and in particular to the instruments of the TBL.

The exposure time is set to 20 msec, which may be too large for speckle applications when the coherence time is smaller than this value. To circumvent this difficulty a rotating shutter was implemented which reduces the exposure time to 5 or 10 msec. This shutter interrupts the light beam in the speckle camera with a rotating opaque sector synchronized with the frame signal of the CP40 (phase-locked motor).

Because of a dead zone between the 4 image quadrants of the CP40, we decided to use only one quadrant and made a special "off-axis" mechanical interface to align the center of the selected quadrant with the optical axis of PISCO.

The geometrical distortion caused by the two-stage amplifier is rather large, of the order of 20% in the edges (Thiebault, 1994).

Another problem is a strongly non-uniform sensitivity of the photo-cathode within a single quadrant (down to nearly zero in one edge), which can hardly be corrected by a flat field map and causes a big non-uniformity of the signal to noise ratio within the elementary frames. The photometry of the image restoration process is also badly affected for intrinsically big objects that spread on the whole image.

The "photon-counting hole" problem with the CP40.

The electronic device which computes the coordinates of the photo-events produces an artifact which affects the photometry of the images.

When two photo-events are very close in the image, they merge into a single spot. The photon centering device is unable to identify it properly and discards such an event. This causes a depletion of high spatial frequencies in the power spectrum. A "hole" can be seen in the center of the mean auto-correlation, which becomes larger when the photon flux increases. This problem also affects the photometry since many photons are not recorded in the high intensity regions of the image.

To reduce this effect during our observations, the photon flux had to be limited to around 10,000 photons/sec and a high magnification was used to over-sample by a factor of 3.

4.2. The Ranicon

The Ranicon ("Resistive Anode camera", described in Clamping and Paresce (1989)) has been built by the Space Telescope Science Institute (Baltimore). The model we used was lent by the Observatoire de la Côte d'Azur (OCA) for some observing runs between 1993 and 1996.

This detector has a S20 photo-cathode and a saturated mode single microchannel amplifier (Gen II). The position analysis of the detected photo-events is made with a resistive anode. Each cloud of amplified electrons, resulting from the impact of a photon on the photo-cathode, produces a charge drift towards the four electrodes which surround the resistive anode. The location of the impact is deduced from the voltage variations at the electrodes and can be measured accurately to about 10 kHz.

Compared to the CP40, the quantum efficiency of the Ranicon is smaller by a factor of ~ 3 . This is due to the lower efficiency of the GEN II compared to the GEN I intensifiers.

Although the micro-channel amplification does not introduce geometric distortion, we have noticed a small distortion with the X and Y axes which are not perfectly perpendicular. A small variation of the geometric scale was also noticed and calibration was needed during the night.

Another unexpected defect was the presence of a small "hole" at the center of the autocorrelation function, similar in some way to that of the CP40 (cf, §4.2), but with a smaller amplitude. This is caused by the depletion of electrons of a micro-channel after a photon-detection: a delay

of a few tenths of milliseconds is needed to recover its full charge and efficiency. To reduce this defect, the photon flux had to be lowered to about 8000 photons/sec.

4.3. Other detectors

Two other detectors have been used with PISCO: the ICCD (Intensified Charge Coupled Device) belonging to C. Aime and E. Aristidi's from Nice University, and P. Nisenson's PAPA camera from Harvard Smithsonian Center for Astrophysics (CfA):

– The ICCD has a single stage intensifier. It cannot operate in true photon counting mode and is thus limited to objects brighter than $V_{lim} \sim 10$. This detector has no significant geometric distortion nor non-linearity problems which would affect the photometry measurements. The exposure time can be set between 64 μ sec and 16 msec and the gain of the micro-channel amplifier can be tuned, thus allowing a wide range of input luminosities. The output is an analog video signal, recorded on SVHS video cassettes. Bispectral image restoration with this detector has been very promising, and the first attempts lead to the restoration of a triple star (Aristidi *et al.*, 1997).

– The principle of the PAPA camera was described in Papaliolios and Mertz (1982) and Papaliolios *et al.*, (1985). It features a two-stage electrostatic amplifier, and a fast (P46) phosphor. Amplified photon impacts are analyzed by a set of binary masks which act as an optical computer to instantly digitize the position of photons in the field. The version we used was new and not fully operational, with a new binary mask setup and a refurbished image intensifier jointly made by P. Nisenson, D. Gezari (CfA) and L. Koechlin (OMP). The first observations in June 1997 have shown that the quantum efficiency was very good, slightly larger than that of the CP40. The maximum photon rate per second was as high as 100,000 but a small “hole” at the center of the autocorrelation function was also noticed. The geometric distortion caused by the image intensifier was large and an overall scale variation during the night imposed quasi permanent scale calibrations. To solve this problem, the image intensifier was changed after these observations.

4.4. Comparison of the detectors

Here is a summary of the characteristics of the detectors used with PISCO.

1. The CP40 has a good quantum efficiency but a non-uniform sensitivity and a strong geometric distortion, with a fixed integration time of 20 msec. The “photon-counting hole” affects the photometry and limits the photon flux to around 10000 ph/sec (limiting magnitude at the TBL: $V_{lim} \sim 12$).
2. The Ranicon has a very low geometric distortion, but a poor quantum efficiency and a limitation of the usable photon flux to around 8000 ph/sec ($V_{lim} \sim 11$). It generates a chronologically ordered list of photon coordinates.
3. The PAPA exhibits a flat-field pattern and geometric distortion. The photon flux is limited to around 100,000 ph/sec, and $V_{lim} \sim 12$. It also a chronologically ordered list of photon coordinates.
4. The ICCD of Nice Univ. has a lower gain than the previous detectors, no geometric distortion, virtually no limitation to the photon flux for normal astrophysical use, and $V_{lim} \sim 10$. The image rate is 50 Hz, with an electronic shutter, able to reduce the integration time to 0.06 msec

Hence the detectors should be chosen according to the observing program, since some defects may be incompatible with the observation requirements. A good detector for high resolution

imaging is still to be desired. Some technical developments are under way in our team to contribute to this problem. A prototype of a new photon-counting camera that would allow a high photon rate and a direct numerisation of photon coordinates is being tested (DELTA camera, Koechlin & Morel, 1998).

5. Performances and limitations

5.1. Physical limitations

The effects of seeing on speckle observations is a strong reduction of the limiting magnitude for bad seeing conditions, whereas the angular resolution attainable in the image restoration process degrades more slowly from the theoretical limit of λ/D , where λ is the wavelength and D is the telescope diameter (Roddier, 1981).

As solar observations have demonstrated, the Pic du Midi site sometimes features slow seeing variations and extended isoplanetic patch, which indicates that the TBL is potentially well suited to speckle and adaptive optics observations at short wavelengths, despite its modest size. With a diffraction limit at 0.06" in V, the TBL can provide high quality data from which many astrophysical programs could benefit.

Due to the necessary short exposure times photon noise is the most severe limiting factor in speckle imaging (Dainty and Greenaway, 1979, Beletic and Goody, 1992). The limiting magnitude depends on the atmospheric seeing, the spectral bandpass, the angular resolution to be achieved, and the quantum efficiency of the detector (Dainty and Greenaway, 1979). We reach $V \sim 12$ with the TBL and detectors such as the CP40 and the PAPA with a bandpass of 70 nm. Without filters, the expected limiting magnitude would increase to about $V \sim 14$. In that case, the wavelength range is determined by the product of the sensitivity response of the detector with that of the photo-cathode, and the resulting bandwidth is a few hundreds of nanometers. It was shown both experimentally (Hege *et al.*, 1981) and with numerical simulations (Ziad *et al.*, 1994) that such extreme observing conditions can be used for faint detection of object duplicity.

5.2. Data processing and image restoration

Whereas data quality is of paramount importance and obviously limits the angular resolution that can be ultimately obtained in the reconstructed images, the nature of the data reduction methods subsequently employed to extract the scientific information contained in these images plays a key role in ensuring the overall success of the scientific programs.

We have written the software to process data from the various detectors used (cf. §4), and the different observing modes: speckle imaging, aperture synthesis with pupil masks, speckle spectroscopy, and coronagraphy. The analysis of the wavefront is not yet implemented.

For speckle imaging, a few observers have independently reached the conclusion that “the bispectrum combined with a constrained iterative deconvolution of amplitudes produces the highest quality imagery” (Beletic and Goody, 1992). Nevertheless, we have used various programs ranging from Knox-Tompson (1974) to full bispectrum methods (Weigelt, 1977, Roddier, 1986, Lannes, 1989) (and even partial bispectrum methods, i.e. using only a subset of all possible closure relations) and found little differences on the restored phasor image of double stars. The pre-processing of the original data (correction of geometric distortion, of flat-field, and various calibrations) is for us the crucial step in the whole image restoration process.

The “Aperture Synthesis” team at OMP has been mainly involved during the last few years in the theoretical aspects of aperture synthesis and related problems such as deconvolution, wavelets and multi-resolution methods, with applications on single aperture interferometry and multi-aperture devices (Lannes *et al.* 1987; Lannes 1988, 1989, 1991). The approach to these problems is deterministic and based on a least-squares scheme that allows error analysis, hence a good understanding of the stability of the image restoration process. Note that the deconvolution

method (Lannes *et al.* 1987) respects the photometry of the target, which is necessary for many applications, such as the determination of color indices of binary stars for example (cf §6).

6. Astrophysical programs

In this section, we describe are some of the scientific subjects which are being studied with PISCO at Pic du Midi. Other programs which aimed at imaging complex objects (asteroids and stellar envelopes) have been impossible to do because of bad weather conditions.

– *Orbits of binary stars*

The study of binaries is a well suited program for speckle cameras as the bibliography of the last two decades can easily show (CHARA project, McAlister and Hartkopf, 1984, 1988, Hartkopf *et al.*, 1996).

A long term program aims at measuring the position of close binaries to determine the orbits and derive the masses of the components using the parallaxes measured by Hipparcos (Carillet *et al.*, 1996, Aristidi *et al.*, 1997, Aristidi *et al.*, 1998). New orbital elements have already been recalculated for 8 double stars from these observations (Aristidi *et al.*, 1998).

We noticed that PISCO was very efficient for binary study, even when the atmospheric conditions were poor and did not allow any other imaging program. Hence binary measurements have been used as a backup program of all our high angular resolution observations.

– *Stellar classification of components of binary stars*

When images have been restored in B, V, R, with a good photometry (cf. §5.2), color indices can be measured which then allow stellar classification of each of the two stars. This may reveal essential for the stars for which a derivation of mass has been made. Accurate orbit determination (and hence masses) are easier to perform for short-period binaries, which are generally very close and for which only global color indices or spectra are available. The individual stellar classification is then poorly known. The paradox is then that accurate masses are affected to stars with big uncertainties in the stellar classification, or less accurate masses to well identified stars, in the case of binaries with a big angular separation. Hence we see that color indices, or even spectra, of individual stars are crucial for stellar studies.

A study of composite spectrum stars (coll. J.-M. Carquillat and N. Ginestet, OMP) associate the imaging and spectroscopic modes of PISCO. Some stars exhibit the signature of a composite spectrum which could be interpreted as the sum of (at least) two spectra of different type. (Ginestet *et al.*, 1994) The aim of this program is to detect the possible presence of a companion and then to identify the spectral type of both components either with color indices or (when possible) with a spectrum with high angular resolution which would separate the spectra of the individual stars.

– *Search for binarity and statistical studies*

The influence of the presence of a companion for star formation (accretion of a disk) and stellar evolution (stellar winds, f.i.) is not yet fully understood. Hence some surveys have been undergone to determine the frequency of binarity among pre-main sequence or post-AGB stars to constrain the theoretical models with these statistical results. Once the binarity has been established, the next step is to identify the nature of each companion, either with its photometry or directly by spectroscopy.

A statistical study of pre-main sequence stars has been started in 1996 with complementary high angular observations made at ESO and CFHT with Adaptive Optics (AO) in the infra-red (Bouvier *et al.*, 1996).

Another program directed by E. Aristidi and B. Lopez (Nice Univ., France) aims at searching for binaries among Mira-type stars (for which binarity has been suspected by Hipparcos), and

studying the interaction between the envelope of the Mira and the atmosphere of the companion (Lopez *et al.*, 1998).

7. Conclusion

The speckle camera of Observatoire Midi-Pyrénées has been tested in all its operating modes and is now qualified for routine scientific exploitation. Its versatility with multi-mode observational possibilities makes it particularly well suited to testing the new methods of image restoration and aperture synthesis. The experience gained with pupil masks may have direct applications for reducing data from optical interferometric arrays.

The good performances of speckle methods for binary star observations have led to consequent orbit measurements during the last twenty years all around the world and PISCO has started to bring its contribution to this effort (Carbillet *et al.*, 1996, Aristidi *et al.*, 1997, Aristidi *et al.*, 1998). This high efficiency makes speckle observations a “privileged” tool for binary studies. A new series of speckle programs have been impelled by the discovery by Hipparcos of thousands of binary candidates (confirmation of binarity, orbits, variability of companions, etc). New space projects such as the space interferometers dedicated to parallax measurements (ESA GAIA) will also need follow-up based-ground observational programs in the future for which PISCO and speckle techniques in general may significantly contribute.

Acknowledgements:

We are indebted to A. Blazit, D. Mourard, E. Aristidi, D. Gezari and P. Nisenson for lending us their detectors, and to A. Lannes, M. Festou, J.-M. Carquillat, N. Ginestet and M. Scardia for the fruitful collaboration for the scientific exploitation of PISCO.

We thank the Observatoire Midi-Pyrénées technical staff, and especially the workshop of Toulouse, Bagnères de Bigorre and Pic du Midi and the night assistants and operators of the TBL, for their participation to this project. We acknowledge the assistance of J. Cadaugade and S. Chastanet for the preparation of the photographs.

This instrument was financed by a grant from the *Institut National des Sciences de l’Univers* of the *Centre National de la Recherche Scientifique (CNRS)* to the TBL, with additional support from the *Unités de Recherche Associées n°1281* and *n°285* (now *Unité Mixte de Recherche n°5572*) of CNRS.

Bibliography

- André, C., Festou, M.C., Koechlin, L., Lannes, A., Perez, J.-P., Prieur, J.-L., Roques, S., 1994, *Planet. Space Sci.*, 42, 747–758.
- Anterrieu, E., 1992, Thesis, Univ. Paul Sabatier, Toulouse, France.
- Aristidi, E., Carbillet, M., Prieur, J.-L., Lopez, B., Bresson, Y., 1997, *A&A Suppl.*, 126, 555.
- Aristidi, E., Prieur, J.-L., Scardia, M., Koechlin, L., Avila, R., Lopez, B., Rabbia, Y., Carbillet, M., Nisenson, P., Gezari, D., 1998, *A&A Suppl.*, accepted.
- Beckers, J.M., Hege, E.K., Murphy, H.P., 1983, *Proc. Soc. Photo-Opt. Instrum. Eng.*, 445, 462.
- Beckers, J.M., Merckle, F., 1991, *Proc. of the ESO conference on: High Resolution Imaging by interferometry II*, Garching, Germany.
- Beletic, J.W., Goody, R.M., 1992, *Applied Optics*, 31, 6909–6921.
- Blazit, A., 1976, Thesis, University of Paris VII, France.
- Blazit, A., 1987, PhD Thesis, University of Nice, France.
- Blazit, A., Bonneau, D., Koechlin, L., Labeyrie, A., 1977, *Astroph. Journ.*, 214, L79–L84.
- Bouvier, J., Corporon, P., Prieur, J.-L., Rigaut, F., Tessier, E., Brandner, W., 1996, in: *Planetary Formation in the Binary Environment*, Stony Brook, 16–18 Juin 1996.
- Breckinridge, J.B., McAlister, H.A., Robinson, W.G., 1979, *Appl. Optics*, 18, 7, 1034–1041.

- Carillet, M., Lopez, B., Aristidi, E., Bresson, Y., Aime, C., Ricort, G., Prieur, J.-L., Koechlin, L., Helmer, G., Lefèvre, J., Cruzalebes, P., 1996, *A&A*, 314, 112.
- Clamping, F., Paresce, F., 1989, *A&A*, 225, 578–584.
- Cuby, J.-G., 1988, *Ann. Phys.*, 13.
- Cuby, J.-G., et al., 1990, *SPIE* 1235, p. 294.
- Dainty, J.C., 1984, in *Topics in Applied Physics, Laser speckle and related phenomena* Vol. 9, (Springer-Verlag) 258–320.
- Dainty, J.C. and Greenaway, A.H., 1979, *JOSA*, Vol. 69, N°5, 786.
- Ginestet N., Carquillat J.M., Jaschek M., Jaschek C., 1994, *A&A Suppl.*, 108, 359–375.
- Golay, M.J.E., 1971, *JOSA*, 61, 272–273.
- Foy R., 1988a, *Speckle Imaging Review*. In: *Instrumentation for ground-based optical astronomy, present and future*, Robinson L.B. (eds), Springer-Verlag (New-York), p345
- Foy R., 1988b, *The Photon-Counting Camera CP40*. In: *Instrumentation for ground-based optical astronomy, present and future*, Robinson L.B. (eds), Springer-Verlag (New-York), p345
- Hege, H.K., Hubbard, E.N., Strittmatter, P.A., Worden, S.P., 1981, *Ap.J.*, 248, L1-L3.
- Hubbard et al. *A.J.*, 84, 1437.
- Knox, K. T., Thomson, B. J., 1974, *Astroph. J.*, 193, L45–L48.
- Koechlin, L., & Morel, S., 1998, *A&A*, accepted.
- Kuwamura, S., Baba, N., Miura, N., Hege, E.K., 1993 *Astron. J.*, 105, 665–671.
- Labeyrie, A., 1970, *A&A*, 6, 85–87.
- Lannes, A., 1988, *Proc. of the NOAO-ESO conference on: High Resolution Imaging by interferometry*, Garching, 169–180.
- Lannes, A., 1989, *Exp. Astron.*, 1, 47–76.
- Lannes, A., 1991, *Inverse Problems*, 7, 261–298.
- Lannes, A., Roques, S., Cazanove, M.J., 1987a, *J. Mod. Optics*, 34, 161–226.
- Lannes, A., Roques, S., Cazanove, M.J., 1987b, *J. Mod. Optics*, 34, 321–370.
- Lopez, B., Aristidi, E., Prieur, J.-L., *et al.*, 1998, in preparation.
- McAlister H.A., Hartkopf W.I., 1984, *Catalog of Interferometric Measurements of Binary Stars*, CHARA contr. n°1, (Georgia State Univ., Atlanta).
- McAlister H.A., Hartkopf W.I., 1988, *Second Catalog of Interferometric Measurements of Binary Stars*, CHARA contr. n°2, (Georgia State Univ., Atlanta).
- Hartkopf, W.I., Mason, B.D., McAlister H.A., Turner, N.H., Barry, D.J., Franz, O.G., Prieto, C.M., 1996 *A.J.*, 111, 936.
- Owens, J.C., 1967, *Applied Optics*, Vol. 6, N°1., 51–59.
- Papaliolios, C., Mertz, L., 1982, *Proc. SPIE*, 331, 360.
- Papaliolios, C., Nisenson, P., Ebstein, S., 1985, *Appl. Optics*, 24, 287–292.
- Prieur, J.-L., Lannes, A., Cullum, M., 1991, *Proc. of the ESO conference on: High Resolution Imaging by interferometry II*, (Ed. J.M. Beckers and F. Merckle) Garching, Germany, 353–357.
- Prieur, J.-L., Festou, M.C, Koechlin, L., André, C., 1994, *Coll. National de Planétologie de l'INSU*, Toulouse, 13–16 Juin 1994, S16-22.
- Richard, J.-C., et al., 1990, *SPIE* 1235, p. 294.
- Roddier, F., 1981, Ed. E. Wolf, *Progress in optics XIX North-Holland*, Vol. 2, p 283.
- Roddier, F., 1986, *Opt. Comm.*, 60, 145–148.
- Roddier, F., & Roddier, C., 1997, *PASP*, 109, 815–820.
- Roques, S., 1987, *Thèse d'Etat*. Univ. Paul Sabatier, Toulouse, France.
- Roggeman, M.C., Welsh, B.M., Fugate, R.Q., 1997, *Rev. of Modern Physics*, Vol 69, 2, 437–505.
- Simon, G.W., 1966, *Astron. J.*, 71, 190.
- Strittmatter, P.A., 1980, in: *Applications of speckle phenomena*, *SPIE*, 243, 103–111.
- Thiebaut, E., 1994, *Thesis*, Univ. Paris VII, France.
- Vernin, J., Roddier, F., 1973, *JOSA*, 63, 270.

Weigelt, G., 1977, *Opt. Comm.*, 21, 55–59.

Weigelt, G, Grieger, F., Hofmann, K.-H., Pausenberger, R., 1991, Colloque ESO. *High Resolution Imaging by interferometry II*, p.471.

Wallner, E.P., Wetherell, W.B., 1990, *Broad spectral bandpass atmospheric dispersion correctors*, Rapport technique Itek.

Ziad, A., Borgnino, J., Agabi, A., Martin, F., 1994, *Exp. Astron.*, 5, 247-268.

